Determining the influence of excited states on current transport in organic light emitting diodes using magnetic field perturbation

Gillin, WP; Zhang, SJ; Rolfe, NJ; Desai, P; Shakya, P; Drew, AJ; Kreouzis, T

Determining the influence of excited states on current transport in organic light emitting diodes using magnetic field perturbation

W. P. Gillin, Sijie Zhang, N. J. Rolfe, P. Desai, P. Shakya, A. J. Drew, and T. Kreouzis
Department of Physics, Queen Mary University of London, Mile End Road, London E1 4NS, United Kingdom
(Received 17 September 2010; revised manuscript received 20 October 2010; published 23 November 2010)

The perturbation of the current transport in aluminum tris(8-hydroxyquinoline) (Alq_3)-based organic light emitting diodes has been investigated as a function of magnetic field. The change in current, or organic magnetoresistance, with applied field has been fitted using two Lorentzian functions corresponding to polaron trapping by triplets and the interaction between polarons and triplets as suggested in the triplet polaron interaction model. The model has been applied to a number of devices with Alq_3 thicknesses from 50 to 90 nm and with two different cathodes. In all cases the data could be fitted using just these two processes, the prefactors for which were found to scale linearly with the triplet population over 6 orders of magnitude. This work demonstrates that the magnitude and shape of the organic magnetoresistance can be predicted and illustrates the importance of magnetic field measurements as a tool for understanding the processes affecting current transport in organic devices.

DOI: 10.1103/PhysRevB.82.195208 PACS number(s): 73.61.Ph, 72.80.Le, 73.43.Qt, 75.47.Pq

There has been an increasing interest in the effects of magnetic fields on the current transport and efficiency in organic devices. It has been known since the 1960s that magnetic fields can influence a number of excitonic processes in organic materials, such as triplet quenching,[1] triplet-triplet annihilation,[2] and intersystem crossing (ISC).[3] In 2003 Kalinowski *et al.*[4] observed that the application of a magnetic field could also perturb the photoconductivity in organic devices and they then showed that for organic light emitting diodes (OLEDs), the application of a weak magnetic field could substantially alter the current in the device as well as its light output[5] and hence its efficiency. Since then the study of these phenomena has increased dramatically[6–36] but there is still no consensus as to the mechanism responsible and there has been little work aimed at successfully predicting the trends observed in the magnetic field effects as the operating conditions of the devices are changed. This is an essential prerequisite for developing a successful model for organic magnetoresistance (OMR).

Although there is a proposed model for OMR in unipolar structures,[34] the majority of the current models are primarily based on the effect of magnetic fields on excitons or the pair states prior to exciton formation.[4,12–14] This is because the majority of experiments suggest that OMR can only be seen in devices above turn-on, i.e., with an applied voltage above the built in potential of the device. The exception to this is for devices that contain a poly(3,4-ethylenedioxythiophene) poly(styrenesulfonate) hole transport layer.[9,21]

The model for OMR that we have proposed in our previous work is based on the effect of excitons (primarily the long-lived triplets) on charge transport.[14] This triplet polaron interaction (TPI) model suggests that triplets can act to reduce the mobility through two mechanisms. The first is through simple trapping and spin blocking. Agranovich *et al.*[37] have demonstrated theoretically that excitons should act as shallow traps for polarons, either through Frenkel-type trapping where the exciton and polaron are on adjacent molecules or through the formation of charged excitons. If a polaron has the same spin state as the corresponding charge carrier on the triplet then the site is spin blocked and only the Frenkel exciton can be formed. This will still affect the mobility of the polaron and this reduction in mobility in the presence of excitons has recently been demonstrated in the polymer system poly-(3-hexylthiophene)[38] and in the small molecule system *N*,*N*′-diphenyl-*N*,*N*′-bis(3-methylphenyl)-(1,1′-biphenyl)-4,4′-diamine (TPD).[39] The second mechanism is that if the spins are opposite, the polaron and triplet can interact to form a charged exciton. Then the triplet acts as a trap for the polaron, much as in the first case, but in addition there are different spin-dependent reactions that can occur which can result in quenching of the triplet.[1] These reactions will also have a magnetic field dependence that should distinguish them from the simple trapping mechanism.

As the triplet population can affect mobility through both trapping and the triplet-polaron interaction, the current in the sample would be expected to show a dependence on magnetic field (due to the field-dependent ISC at either the pair-state or excitonic level[3,14,40]), and this would be expected to scale with the absolute triplet concentration. Not only would the magnitude of the process be expected to scale with the triplet population but the magnetic field dependence of the trapping component should mirror any change in the triplet population. It is worth noting that the increase in current attributed to the trapping component should also have the same saturation field as the change in efficiency. Perhaps more interestingly, the magnitude of both mechanisms should scale with absolute exciton concentration. In this paper, we show that this is indeed the case.

OLED devices consisted of a patterned indium-tin-oxide (ITO) coated glass substrate on to which was grown a 50 nm layer of TPD as the hole transport layer, followed by a 50, 70, or 90-nm-thick layer of aluminum tris(8-hydroxyquinoline) (Alq_3) as an electron transport/emissive layer and a LiF (1 nm)/Al (100 nm) or Al (100 nm) cathode. All organic materials were purified by vacuum sublimation prior to use. Final device areas were ~ 4 mm^2. The ITO substrates were patterned using photolithography and

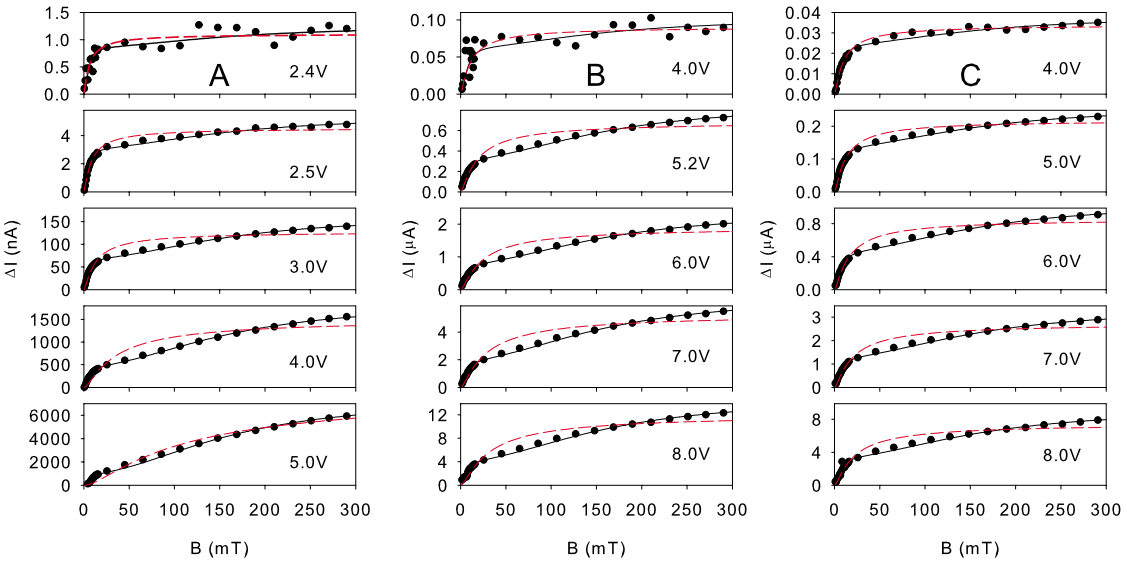

FIG. 1. (Color online) The absolute change in current in (A) a 50 nm, (B) a 70 nm, and (C) a 90 nm Alq_3 OLED with applied magnetic field for several drive voltages. The fits to the curves were obtained using Eq. 3 and the parameters in the text. The dashed fits are obtained by free fitting with the specific "non-Lorentzian" function $B^2/(|B|+B_0)^2$.

cleaned by ultrasonicating in detergent/water, acetone and chloroform. Following this the ITO was treated in an oxygen plasma for 5 min at 30 W and 2.5 mbar pressure using a Diener Electronic Femto plasma system. The plasma treated substrate was immediately transferred to the deposition chamber for device fabrication. The deposition of the organic layers and metal electrodes were performed using a Kurt J. Lesker SPECTROS evaporation system with a base pressure during evaporation of $\sim 10^{-7}$ mbar. The rate of deposition of organic materials was about 0.2 nm/s while that of the aluminum was varied from ~0.1 to 1 nm/s. A calibrated oscillating quartz-crystal monitor was used to determine the rate and thickness of the deposited layer. The whole device fabrication was performed without breaking vacuum.

Immediately after growth the devices were placed in a light-tight sample holder with a calibrated silicon photodetector (Newport 818-SL), whose output is field independent, placed on the top surface of the device. The sample holder was placed between the poles of an electromagnet with the magnetic field perpendicular to the direction of current flow in the device. 32 independent measurements were taken and then averaged with the device operated in vacuum and in constant voltage mode. Before and after each field measurement, a measurement at null field was taken and used to remove any effects due to drifting in the device characteristics. The measurements were performed using a Keithley 236 source-measure unit and Newport 1830 optical power meter.

Figure 1(a) shows the OMR curves (plotted as the absolute change in current) for a 50 nm Alq_3 device as a function of drive voltage. Below 2.4 V there was no OMR, which is the voltage at which light output can be observed. This is the same as we have observed in all our previous work[14] and strongly suggests an excitonic cause behind the OMR. At 2.4 V the OMR has an approximately Lorentzian shape of the form $f(B) \sim B^2/(B^2+B_0^2)$, where B is the applied magnetic field and a saturation field of $B_0 \sim 6$ mT, which was first noticed by Mermer *et al.*[9] The Lorentzian line shape has been shown to be a solution to the Hamiltonians for both hyperfine[10] and spin-orbit[19] interactions, and as such may be a generic expression for a spin interaction in the presence of a magnetic field in these systems. Although Mermer also used an empirical equation $B^2/(|B|+B_0)^2$ in his work, which gives an excellent fit to our data at voltages just above turn on, we found that for all other voltages, regardless of device thickness or cathode composition, this empirical equation was a poor fit to the data. This empirical equation has been shown to have an analytical origin in the bipolaron model of OMR.[41]

As we have already suggested, there are two independent processes occurring in the OMR,[14] simple trapping at excitons and TPIs. We have therefore tried to fit our data using two Lorentzian functions with different saturation fields (shown by the lines in Fig. 1). The low-saturation field component in the OMR is due to the simple trapping of charges at excitons predicted by Agranovich *et al.*[37] and the higher field process is the triplet polaron interaction process observed by Ern and Merrifield[1] in anthracene. The simple trapping (low-field) component should mirror the change in concentration of triplets caused by ISC at either the excitonic or pair-state level. It is this process that is responsible for the change in efficiency observed in these devices and hence this component should show the same magnetic field dependence as the efficiency. The magnetic field effect on the efficiency for the three devices is shown in Fig. 2. The fits to this data are single Lorentzian with an average B_0 value of 5.5 mT. The higher field component is due to the interaction of triplets with polarons and the only data for the magnetic field dependence of this is the change in triplet lifetime with magnetic field observed by Ern and Merrifield[1] in anthracene. Ern and Merrifield's data are replotted in Fig. 3 and the solid lines are again a single Lorentzian fit. For anthrancene the B_0 value for this triplet polaron interaction was found to be ~70 mT, which is a much larger field scale than that for ISC component.

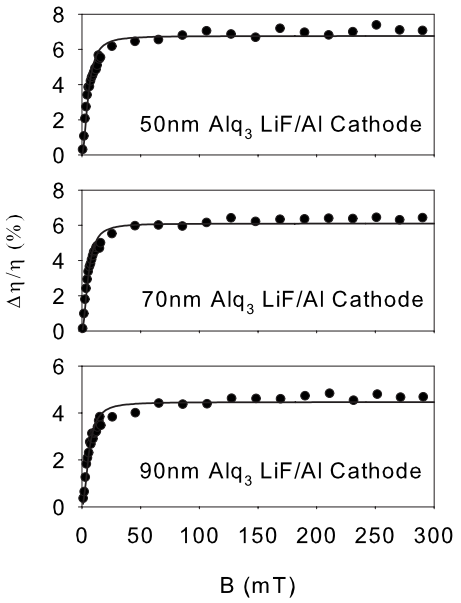

FIG. 2. Percentage change in efficiency for the 50, 70, and 90 nm Alq_3 devices with LiF/Al cathodes. The fits are single Lorentzians and the B_0 values for the three fits are 5.4 mT, 5.3 mT, and 5.9 mT for the 50 nm, 70 nm, and 90 nm devices, respectively.

To fit all the data from this device as a function of operating voltage we have therefore used this combination of two Lorentzians for the exciton trapping and interaction components to fit our OMR data. Initially we performed free fits to the data, producing excellent fits to the low- and high-field components. The low component had an average value of 5.6 ± 1.6 mT, which is very similar to the value obtained from a single lorentzian fit to the efficiency data. For the high-field component, we found that it saturated at $\sim 160 \pm 20$ mT at higher operating voltages, where the process becomes dominant. Since there are only two processes

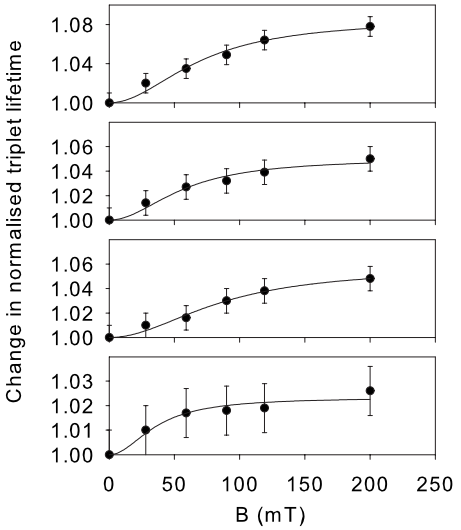

FIG. 3. The magnetic field dependence of the normalized triplet lifetime in x-ray-irradiated anthracene, extracted from the work of Ern and Merrifield (Ref. 1). The solid lines are a Lorentzian fit to the data.

operating, which are fundamental to the properties of Alq_3, we fitted all of the data with constrained values. The final function used for the fit was therefore,

$$f(B) = a_t \frac{B^2}{(B^2 + B_t^2)} + a_i \frac{B^2}{(B^2 + B_i^2)},$$

where B is the applied magnetic field, a_t an a_i are the prefactors for the Lorentzians, and B_t and B_i are the saturation fields, the subscripts t and i stand for trapping and interaction, respectively. The constraints used in the fit were $a_t > 0$,

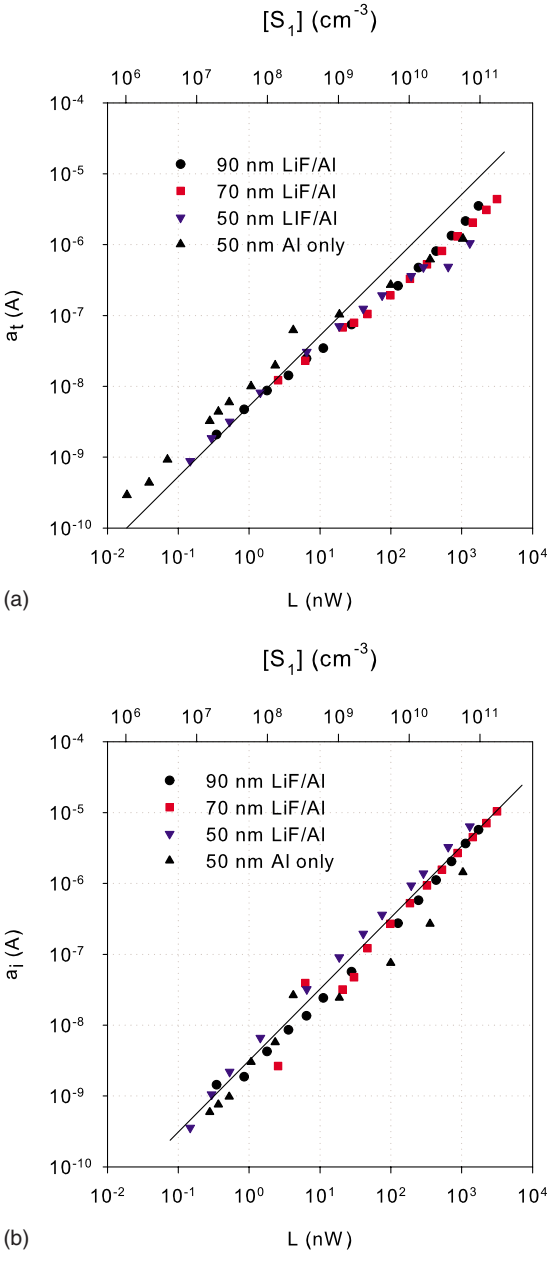

FIG. 4. (Color online) The prefactors from the fits plotted against light output. (a) shows the exciton trapping component, a_t and (b) shows the TPI component, a_i. The upper axis shows the singlet concentration calculated assuming all the excitons are in a layer 30 nm thick in all devices and monochromatic light emission at 520 nm. The straight lines are of slope 1.

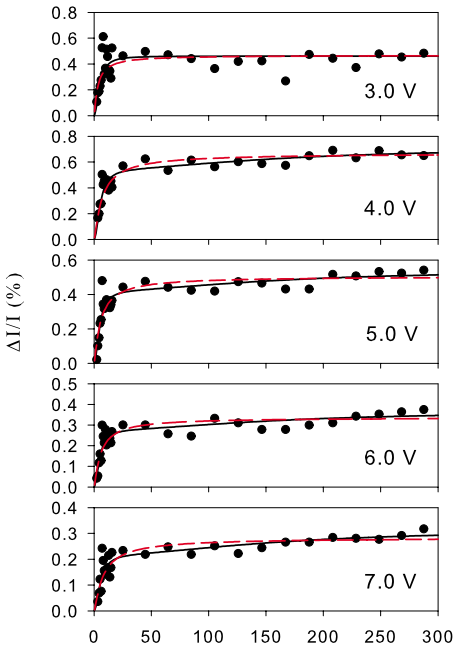

FIG. 5. (Color online) The percentage change in current with applied magnetic field for a 50 nm Alq_3 OLED with an aluminum only cathode at several drive voltages. The fits to the curves were obtained using Eq. 3 and the parameters in the text. The dashed fits are obtained by free fitting with the specific non-Lorentzian function $B^2/(|B|+B_0)^2$.

$5<B_t<7$ mT, $a_i>0$, and $B_i=160$ mT. A selection of the OMR data and the resultant fits are shown in Fig. 1 and the data and fits for all devices at all voltages (~50 data sets) can be found in the supplementary material.[42] As can be seen, the quality of the fits is excellent in all cases.

In Figs. 1(b) and 1(c) the data and fits, using the same constraints, are also shown for 70 and 90 nm Alq_3 devices. From all of the data measured, which includes over 50 OMR curves measured over a wide range of operating voltages, currents, and material thicknesses, the results can be fitted using just two processes, the exciton trapping and TPI terms. For all data in all devices, the saturation fields for the two processes were constrained and the only fitting parameters were the prefactors for the two Lorentzians.

These results clearly demonstrate that over a range of device thicknesses and operating voltages the OMR data can be described by considering the magnetic field dependence of the singlet-triplet ISC rate, which modifies the triplet concentration, and the TPI. Although we refer here to ISC the exchange between singlets and triplets can occur at both the exciton and pair-state level.[40] The effect of the magnetic field on the ISC rate has two effects, first it is responsible for the changes in device efficiency that we have previously reported in a number of devices,[14–16] second by changing the concentration of triplets it can affect the magnitude of the polaron trapping and hence affect the mobility.[39] Given that the change in mobility, and hence the current through the device, caused by either of these processes should be dependent on the triplet concentration, we have plotted in Fig. 4 the prefactors for the two Lorentzians against the luminescence intensity from the devices. The luminescence intensity

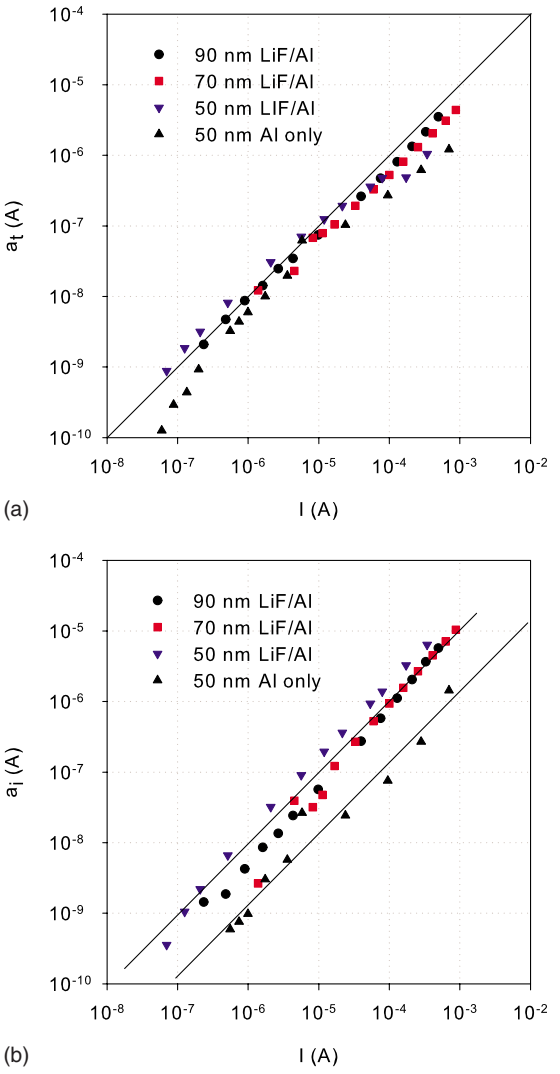

FIG. 6. (Color online) The prefactors from the fits plotted against current through the device. (a) shows the exciton trapping component, a_t and (b) shows the TPI component, a_i. The straight lines are of slope 1.

is a direct measure of the singlet concentration, also shown in Fig. 4, and will be directly proportional to the triplet concentration in our devices. From Fig. 4 it can be seen that for all device thicknesses the magnitude of the two components scale linearly with exciton concentration. As the magnitude of the prefactors for the two OMR processes depend on the exciton concentration, and hence are proportional to the light output, devices with different efficiencies should give identical results. We therefore performed the same analysis on a 50 nm Alq_3 device with an aluminum only cathode, rather than the LiF/Al cathode normally used. These devices have an efficiency approximately an order of magnitude lower and yet, as can be seen from Fig. 4, there is excellent agreement between all the data. This is irrespective of device thickness or cathode used. It is worth noting that for the aluminum cathode only device the OMR curves are reasonably well fitted with the empirical non-Lorentzian curves although the curves are much better described by the dual Lorentzian fit (Fig. 5). We have seen that for all our devices the more

efficient they are the greater the magnitude of the TPI component that is present in the OMR curves. This suggests that the empirical non-Lorentzian fit may just be an approximation to a two Lorentzian process when the magnitude of the high-field component is small.

Although the bipolaron model, in its original form,[34] does not explain the change in shape of the OMR with operating conditions, it would predict an effect that scales with current density rather than exciton concentration. As the light output from our devices is a linear function of the current density, the data for the Al only cathode device which has a much lower efficiency provides a good comparative test of the two models. Under the bipolaron model the magnitude of any process responsible for the OMR would be expected to scale with current rather than exciton concentration. This is shown in Fig. 6. For the trapping component of our fit, the Al only data are consistently lower than that for the LiF/Al cathode data but this difference is relatively small. For the Al only cathode the magnitude of the interaction component data is an order of magnitude lower than for the LiF/Al cathode data. This reduction strongly suggests that the bipolaron model is not responsible for OMR. However, there is a good correlation between exciton concentration and the magnitude of both the TPI and trapping components for all device thicknesses and materials (Fig. 4). This is strong evidence that the effects are dependent on an excitonic model, such as the TPI and trapping models discussed above. We note that none of the alternative models of OMR have been shown to predict how OMR changes with drive conditions. Neither can they explain the changes in shape that are frequently seen in OMR data for a given device, as the drive voltage and current are changed.

In conclusion, our approach shows that not only does the OMR scale linearly over the range of operating voltages for our devices but also that the observed change in shape of the OMR can be modeled using only two processes which scale independently with exciton concentration. The two primary mechanisms are polaron trapping at triplets and triplet-polaron interaction. Both have been theoretically predicted[1,37] and the effect of excitons[38] and magnetic field on mobility[38,39] have been measured independently using the dark injection method. The magnetic field dependence of the polaron trapping processes is identical to the change in efficiency, caused by a change in the intersystem crossing rate between singlets and triplets which could occur at either the excitonic or pair-state level.[40] The magnetic field dependence of the interaction process is also Lorentzian, although measurements to higher magnetic fields will be required to fix the precise value for the saturation field. The observation that the triplet-polaron interaction is Lorentzian is consistent with Ern and Merrifield's work on triplet quenching in anthracene.[1,42]

[1] V. Ern and R. E. Merrifield, Phys. Rev. Lett. **21**, 609 (1968).
[2] R. C. Johnson and R. E. Merrifield, Phys. Rev. Lett. **19**, 285 (1967).
[3] R. P. Groff, A. Suna, P. Avakian, and R. E. Merrifield, Phys. Rev. B **9**, 2655 (1974).
[4] J. Kalinowski, J. Szmytkowski, and W. Stampor, Chem. Phys. Lett. **378**, 380 (2003).
[5] J. Kalinowski, M. Cocchi, D. Virgili, P. Di Marco, and V. Fattori, Chem. Phys. Lett. **380**, 710 (2003).
[6] A. H. Davis and K. Bussmann, J. Vac. Sci. Technol. A **22**, 1885 (2004).
[7] T. L. Francis, O. Mermer, G. Veeraraghavan, and M. Wohlgenannt, New J. Phys. **6**, 185 (2004).
[8] O. Mermer, G. Veeraraghavan, T. L. Francis, and M. Wohlgenannt, Solid State Commun. **134**, 631 (2005).
[9] O. Mermer, G. Veeraraghavan, T. L. Francis, Y. Sheng, D. T. Nguyen, M. Wohlgenannt, A. Kohler, M. K. Al-Suti, and M. S. Khan, Phys. Rev. B **72**, 205202 (2005).
[10] Y. Sheng, T. D. Nguyen, G. Veeraraghavan, O. Mermer, M. Wohlgenannt, S. Qiu, and U. Scherf, Phys. Rev. B **74**, 045213 (2006).
[11] H. Odaka, Y. Okimoto, T. Yamada, H. Okamoto, M. Kawasaki, and Y. Tokura, Appl. Phys. Lett. **88**, 123501 (2006).
[12] V. N. Prigodin, J. D. Bergeson, D. M. Lincoln, and A. J. Epstein, Synth. Met. **156**, 757 (2006).
[13] Y. Wu and B. Hu, Appl. Phys. Lett. **89**, 203510 (2006).
[14] P. Desai, P. Shakya, T. Kreouzis, W. P. Gillin, N. A. Morley, and M. R. J. Gibbs, Phys. Rev. B **75**, 094423 (2007).
[15] P. Desai, P. Shakya, T. Kreouzis, and W. P. Gillin, J. Appl. Phys. **102**, 073710 (2007).
[16] P. Desai, P. Shakya, T. Kreouzis, and W. P. Gillin, Phys. Rev. B **76**, 235202 (2007).
[17] B. Hu and Y. Wu, Nature Mater. **6**, 985 (2007).
[18] F. L. Bloom, W. Wagemans, M. Kemerink, and B. Koopmans, Phys. Rev. Lett. **99**, 257201 (2007).
[19] Y. Sheng, T. D. Nguyen, G. Veeraraghavan, O. Mermer, and M. Wohlgenannt, Phys. Rev. B **75**, 035202 (2007).
[20] Y. Wu, Z. Xu, B. Hu, and J. Howe, Phys. Rev. B **75**, 035214 (2007).
[21] T. D. Nguyen, Y. Sheng, J. Rybicki, G. Veeraraghavan, and M. Wohlgenannt, J. Mater. Chem. **17**, 1995 (2007).
[22] J. D. Bergeson, V. N. Prigodin, D. M. Lincoln, and A. J. Epstein, Phys. Rev. Lett. **100**, 067201 (2008).
[23] F. J. Wang, H. Bassler, and Z. V. Vardeny, Phys. Rev. Lett. **101**, 236805 (2008).
[24] N. Rolfe, P. Desai, P. Shakya, T. Kreouzis, and W. P. Gillin, J. Appl. Phys. **104**, 083703 (2008).
[25] P. Shakya, P. Desai, T. Kreouzis, W. P. Gillin, S. M. Tuladhar, A. M. Ballantyne, and J. Nelson, J. Phys.: Condens. Matter **20**, 452203 (2008).
[26] P. Shakya, P. Desai, T. Kreouzis, and W. P. Gillin, J. Appl. Phys. **103**, 043706 (2008).
[27] P. Shakya, P. Desai, M. Somerton, G. Gannaway, T. Kreouzis, and W. P. Gillin, J. Appl. Phys. **103**, 103715 (2008).
[28] T. H. Lee, T. F. Guo, J. C. A. Huang, and T. C. Wen, Appl. Phys. Lett. **92**, 153303 (2008).
[29] C. G. Yang, E. Ehrenfreund, F. Wang, T. Drori, and Z. V. Vardeny, Phys. Rev. B **78**, 205312 (2008).
[30] T. D. Nguyen, J. Rybicki, Y. Sheng, and M. Wohlgenannt, Phys. Rev. B **77**, 035210 (2008).

[31] T. D. Nguyen, Y. Sheng, J. Rybicki, and M. Wohlgenannt, Phys. Rev. B **77**, 235209 (2008).
[32] F. L. Bloom, W. Wagemans, and B. Koopmans, J. Appl. Phys. **103**, 07F320, (2008).
[33] F. L. Bloom, W. Wagemans, M. Kemerink, and B. Koopmans, Appl. Phys. Lett. **93**, 263302 (2008).
[34] P. A. Bobbert, W. Wagemans, F. W. A. van Oost, B. Koopmans, and M. Wohlgenannt, Phys. Rev. Lett. **102**, 156604 (2009).
[35] L. Xin, C. Li, F. Li, S. Liu, and B. Hu, Appl. Phys. Lett. **95**, 123306 (2009).
[36] N. J. Rolfe, M. Heeney, P. B. Wyatt, A. J. Drew, T. Kreouzis, and W. P. Gillin, Phys. Rev. B **80**, 241201 (2009).
[37] V. M. Agranovich, D. M. Basko, K. Schmidt, G. C. LaRocca, F. Bassani, S. Forrest, K. Leo, and D. Lidzey, Chem. Phys. **272**, 159 (2001).
[38] J. Y. Song, N. Stingelin, W. P. Gillin, and T. Kreouzis, Appl. Phys. Lett. **93**, 233306 (2008).
[39] J. Y. Song, N. Stingelin, A. J. Drew, T. Kreouzis, and W. P. Gillin, Phys. Rev. B **82**, 085205 (2010).
[40] S. Zhang, J. Y. Song, T. Kreouzis, and W. P. Gillin, J. Appl. Phys. **106**, 043511 (2009).
[41] P. A. Bobbert, T. D. Nguyen, W. Wagemans, F. W. A. van Oost, B. Koopmans, and M. Wohlgenannt, Synth. Met. **160**, 223 (2010).
[42] See supplementary material at http://link.aps.org/supplemental/10.1103/PhysRevB.82.195208 for OMR curves and fits for all the data presented in the manuscript.